Universidad de La Laguna

Facultad de Ciencias

Expanding the horizons of Tm^{3+} temperature sensing in the context of biological applications

Trabajo de Fin de Grado

Author

Micaela C. Domínguez Crosa

Tutors:

Inocencio Rafael Martín Benenzuela

Kevin Soler Carracedo

July 2024

Contents

Para Elisa

1 Abstract

El objetivo principal de este trabajo es estudiar la viabilidad de usar $Gd_3NbO_7 : Yb^{3+}, Tm^{3+}$ *mezclado en una resina Simple Siraya Tech, generalmente utilizada en la impresión 3D, como un sensor de temperatura remoto mientras se encuentra sumergido en dos fluidos diferentes: 2-Propanol y agua.*

El material ópticamente activo se sintetiza con éxito y se mezcla con la resina Simple Siraya Tech, creando una muestra que se estudia para determinar sus capacidades de detección térmica. Las bandas de emisión en 1626 nm, 1436 nm y 831 nm obtenidas cuando la muestra se excita con un láser de 700 nm corresponden a las siguientes transiciones de los iones Tm^{3+}*: 3F4 → 3H6, 3H4 → 3F4 y 3H4 → 3H6, respectivamente. Se utilizan para aplicar la técnica Luminiscencia Intensity Ratio (LIR) para niveles no termalizados (non-TCLs).*

La muestra se sumerge en 2-propanol y se excita con un láser de 700 nm; Se detectan las bandas de emisión a 1626 nm y 1436 nm para medir el desempeño del sensor utilizando la técnica LIR en un rango de temperatura entre aproximadamente 21^oC *y* 50^oC*. Se calcula la Sensitividad Térmica Relativa* S_{Rel} *y la incertidumbre de la temperatura* δT*.*

De manera similar, se procede a medir LIR cuando la muestra está inmersa en agua. Sin embargo, se mide la emisión a 831 nm en lugar de la

emisión a 1436 nm, utilizando excitación y emisiones que caen dentro de las ventanas biológicas (BW-I y BW-III). Se calcula el LIR experimental en un rango de temperatura aproximado de 21ºC a 50ºC y posteriormente se ajusta. Se calcula la Sensitividad Térmica Relativa S_{Rel} y la incertidumbre de la temperatura δT.

Se observa una disminución en la intensidad de las emisiones a 1436 y 1626 nm cuando la muestra está sumergida en agua en comparación con la intensidad observada cuando está inmersa en 2-propanol, debido a la absorción del agua.

Cabe mencionar que, según nuestro conocimiento, esta es la primera vez que los non-TCLs de Tm^{3+} utilizados en ambos experimentos de este trabajo han sido analizados en función de la temperatura.

The main objective of the present work is to study the feasibility of using a $Gd_3NbO_7 : Yb^{3+}, Tm^{3+}$ mixed in a Simple Siraya Tech resin, usually utilized in 3D printing, as a remote temperature sensor while it is immersed in two different fluids, 2-Propanol and water.

The optical active material is successfully synthesized and mixed the with resin, creating a sample which is studied in order to determine its thermal sensing capabilities. The emission bands in 1626 nm, 1436 nm and 831 nm obtained when the sample is excited with a 700 nm laser corresponding with the following transitions of the Tm^{3+} ions: $^3F_4 \rightarrow ^3 H_6$, $^3H_4 \rightarrow ^3 F_4$ and

$^3H_4 \rightarrow ^3 H_6$, respectively. They are used to apply LIR technique for non-Thermally Coupled Levels.

The sample is immersed in 2-propanol and excited with a 700 nm laser, where the emission bands at 1626 nm and 1436 nm are detected to measure the performance of the sensor using the Luminescence Intensity Ratio technique for a temperature range between approximately 21ºC and 50ºC. It is calculated the Relative Thermal Sensitivity (S_{Rel}) and Temperature Uncertainty δT.

In a similar way, it is proceeded to measure LIR when the sample when the sample immersed in water. Yet, the emission at 831 nm is measured instead of the emission at 1436 nm, using excitation and emissions that fall within biological windows (BW-I and BW-III). It is calculated the experimental LIR in a temperature range between approximately 21ºC and 50ºC and it is later fitted. It is calculated the Relative Thermal Sensitivity (S_{Rel}) and temperature uncertainty δT.

It is observed a decrease in intensity for the 1436 and 1626 nm emissions when the sample is submerged in water versus when it is immersed in 2-Propanol, attributed to water absorbance.

It is worth to mention that, in the best of our knowledge, this is the first time the Tm^{3+} non-TCLs used in both of our experiments have been analyzed as a function of temperature.

2 Introduction

En esta sección, se enmarca el objetivo principal de este trabajo dentro de la actualidad del mundo de la investigación; Se detalla la relevancia de la luminiscencia de los lantánidos, especialmente los sensores remotos de temperatura y, en concreto, se insiste en la importancia que tienen en aplicaciones biológicas, comparándolos con otros tipos de termómetros y tratando sus ventajas y desventajas respecto a estos; Finalmente, se presentan las propiedades que convierten a los termómetros basados en lantánidos, particularmente el $Gd_3NbO_7 : Yb^{3+}, Tm^{3+}$ *insertado en resina, en una buena alternativa dentro de una gran variedad de aplicaciones*

Lanthanide luminescence is central to a wide range of applications including lighting, telecommunications, lasers, security marking, barcoding, optical medical imaging, immunoassays and luminescent sensing, among others[1]. The ability of lanthanide-doped materials to provide accurate and rapid temperature measurements makes them invaluable in many fields.

Temperature is a critical physical parameter for many industrial, biological and medical processes[2]. Accurate, precise, and rapid temperature measurement is particularly important in nanomedicine and diagnostics because many physiological processes, such as cell division, gene expression, and enzyme activity, are temperature dependent. In addition, certain pathological conditions, such as cancer pathogenesis, often involve localized heat production[3].

Traditional temperature sensors are typically contact-based, requiring direct physical contact of an invasive probe with the subject to obtain a thermal reading. These sensors have significant limitations, including invasiveness, potential disruption of the experimental conditions, and only surface-level temperature measurement[3].

The demand for non-invasive, remote temperature sensors has driven interest in lanthanide-doped luminescent thermometers. These thermometers

offer rapid and accurate temperature readings and can be excited and emit within the Biological Windows (BW-I: 650-950 nm, BW-II: 1000-1350 nm, BW-III: 1500-1800 nm)[4], which is ideal for biomedical applications due to their deep tissue penetration capabilities[3].

However, water exhibits strong absorption bands ($\alpha_{\text{abs}} > 0.25$ cm^{-1}) at 980 nm, 1150 nm, and 1500 nm, which, indeed, define the boundaries of the biological windows[5]. These absorption bands pose a significant challenge for ratiometric luminescent thermometers operating in the second biological window (NIR-II, 1000-1500 nm). Additionally, tissue scattering becomes predominant over absorption at wavelengths shorter than 650nm, resulting in wavelength-dependent tissue transmission in the visible range[5].

In this work, we evaluate the feasibility of using lanthanide-doped resin with Tm^{3+} and Yb^{3+} for temperature measurement in 2-Propanol and water, two fluids frequently used in many biological solutions and processes, over a temperature range of approximately 21-50°C. The thermal sensing capabilities of the material were evaluated using the Luminescence Intensity Ratio (LIR) technique for non-thermally coupled levels (non-TCLs) between the 831, 1436, and 1626 nm emissions of the Tm^{3+} ion. Lanthanide-doped luminescent thermometers can be fabricated by incorporating these elements into resins used in 3D printing. This approach enables temperature measurement without the need for additional contact equipment, providing a seamless integration into the system where the 3D printed piece is deployed[6].

3 Aim of this work

Se hace conocer que el objetivo principal de este trabajo es analizar la viabilidad de utilizar $Gd_3NbO_7 : Yb^{3+}, Tm^{3+}$ mezclado con una resina Simple Siraya Tech, comúnmente utilizada en impresión 3D, como sensor remoto de temperatura en dos medios diferentes: 2-Propanol y agua; Y los pasos seguidos para conseguir esta meta.

The primary objective of this study is to investigate the feasibility of $Gd_3NbO_7 : Yb^{3+}, Tm^{3+}$ embedded in Simple Siraya Tech resin, commonly used in 3D printing, as a remote temperature sensor when immersed in two different fluids: 2-Propanol and water. To achieve this objective, the following tasks will be undertaken:

- Incorporate the optically active material $Gd_3NbO_7 : Yb^{3+}, Tm^{3+}$ into Simple Siraya Tech resin to create a remote temperature sensor.
- Examine the emission of the doped sample at 831 nm, 1436 nm, and 1626 nm under excitation with a 700 nm laser.
- Measure the emission of the sample as a function of temperature and use LIR technique focusing on ratio between the emissions at 1436 nm ($^3H_4 \rightarrow ^3 F_4$) and 1626 nm ($^3F_4 \rightarrow ^3 H_6$) while immersed in 2-Propanol.
- Measure the emission of the sample as a function of temperature and use LIR technique focusing on ratio between the emissions at 831 nm ($^3H_4 \rightarrow ^3 H_6$) and 1626 nm ($^3F_4 \rightarrow ^3 H_6$) while immersed in water.
- Evaluate the performance of the sensor by comparing the intensity ratios of the emissions at 1626 nm and 1436 nm with the intensity ratios of the emissions at 1626 nm and 831 nm to determine the optimal configuration for biological applications.

4 Theoretical background

En la sección actual, se desarrollan las bases teóricas que se debe conocer para entender cómo funcionan los termómetros basados en la luminiscencia de los lantánidos; Concretamente, se habla sobre el método LIR para niveles no termalizados (non-TCLs) y la evaluación del desempeño de los termómetros ratiométricos.

4.1 Rare-Earth Ions: Thulium and Ytterbium

In their ground state, rare-earth elements have an electronic configuration that consists of a core identical to that of Xenon plus additional electrons in higher orbits[7]. Thulium (Tm) and Ytterbium (Yb) are lanthanides, a kind of rare-earth elements, and their electronic configuration in the ground state is:

$$\begin{aligned} \text{Tm} &: ... \ 4f^{13} \ 5s^2 \ 5p^6 \ 6s^2 \\ \text{Yb} &: ... \ 4f^{14} \ 5s^2 \ 5p^6 \ 6s^2 \end{aligned}$$

The first nine shells and subshells up to $4d^{10}$ are completely filled. Therefore only the outer electron configuration is given.

Rare-earth ions have a special place in photonics because of their unique photophysical properties, particularly in the generation and amplification of light. They present a wide variety of sharp fluorescent transitions representing almost every region of the visible and near-infrared parts of the electromagnetic spectrum. These ions are normally trivalent, and its luminescence spectra arises from the partially filled $4f$ shell, which is shielded by the filled $5s$ and $5p$ outer shells. For Tm and Yb[7][8]:

$$\begin{aligned} \text{Tm}^{3+} &: ... \ 4f^{12} \ 5s^2 \ 5p^6 \\ \text{Yb}^{3+} &: ... \ 4f^{13} \ 5s^2 \ 5p^6 \end{aligned}$$

Electrons present in the $4f$ shell can be risen by light absorption into unoccupied $4f$ levels, producing luminescence as the result of the competition of radiative and non-radiative pathways in the relaxation of the electronically excited species[7][8].

Due to this, when a rare-earth ion is successfully introduced into a particular material, it will become luminescent. Because of the shielding effect of the outer electrons, its emission lines ions will vary only slightly from one host to another[7][8].

4.2 Luminescence thermometers

Luminescence is mostly referred as the spontaneous emission of light that is not the result of a heating process. The emission of luminescence occurs after a suitable material has absorbed energy[9].

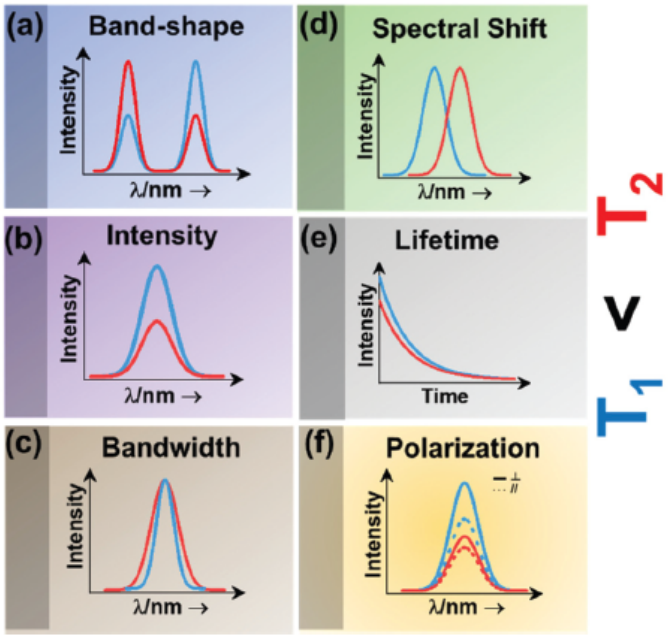

Figure 1: Parameters used for luminescent sensing[3][9].

Luminescence thermometry is the relationship between temperature and the luminescent properties of the light emitted by certain elements. Due to the temperature changes, different luminescent characteristics may change. These include the change in bandshape (a), intensity of emission (b), bandwidth (c), spectral shift (d), lifetime (e) and polarization (f) [3][9], as observed in Fig.1.

Lanthanides possess several characteristics that make them suitable for temperature sensing applications, such as the presence of thermally coupled emitting levels (as well as luminescence covering most of the UV-VIS-NIR spectra), high quantum yield, sharp emission lines, and the possibility for energy down- and up- conversion, among others[3][10].

Lanthanide-based inorganic compounds, such as fluorides, oxides, vanadates and phosphates are the most used materials in luminescence thermometry. These compounds are made of a host or matrix, which is often thermally stable and has relatively low phonon energies, so it can allow the development of highly efficient phosphors and might exhibit a strong photoluminescence signal. These hosts are embedded with a molecule or activator ion, a Lanthanide (Ln^{3+}), which is an optically active specie (e.g., Eu^{3+}, Tb^{3+}, Nd^{3+}, Er^{3+}, Tm^{3+}). Sometimes, this activator is accompanied by a sensitizer (predominantly Ce^{3+} and Yb^{3+}) which usually improves the capability of absorbing light and source the activator ion that in the end will generate luminescence[3][10].

4.2.1 Luminescence Intensity Ratio (LIR)

As formerly stated, temperature can produce changes in the intensity of the luminescence bands of the substance. These changes are related to the thermal activation of quenching processes and an increase in the probability of non-radiative mechanisms.

Luminescence Intensity Ratio, or LIR (also found in literature as Fluorescence Intensity Ratio, FIR) is a technique based in the previous changes in intensity defined by:

$$LIR \ = \ \frac{I_2}{I_1} \tag{1}$$

Where I_2 and I_1 can be either the value of the maximum intensity values or the integrated area of the corresponding emissions[3][11].

LIR or FIR technique is traditionally applied mostly to Thermally Coupled Levels (TCL), which follows a Boltzmann type-distribution. Yet, it can also be calculated for non-Thermally coupled Levels (non-TCLs), but the calibration must be made using different dependencies[3][11].

4.2.2 Sensor performance

Regardless of the class of luminescent thermometry used to extract temperature information, thermal sensitivity can be used to evaluate and compare the performance of a lanthanide-doped thermometer, as well as that of other thermometers based on other materials.

On one side, the absolute thermal sensitivity (S_{abs}) can be used. It is defined as:

$$S_{abs} \ = \ |\frac{\partial LIR(T)}{\partial T}| \tag{2}$$

Where S_{abs} is expressed in K^{-1} (or $^{o}C^{-1}$) and, as it is heavily related to the experimental setup and sample characteristics, is restricted to comparing only thermometers of the same nature and tested under the same conditions[3][9].

Moreover, if the aim is to compare thermometers independently of their nature or material employed, the relative thermal sensitivity (S_{rel}) must be used. S_{Rel} expresses the maximum change in LIR for each temperature degree and it is defined as:

$$S_{Rel} \ = \ \frac{1}{LIR}|\frac{\partial LIR(T)}{\partial T}|\text{x}100 \tag{3}$$

Where S_{rel} is expressed in units of % change per degree of temperature change (% K^{-1} or $\%^{o}C^{-1}$). High relative thermal sensitivity is considered in cases where $S_{rel} > 1\%^{o}C^{-1}$[3][9].

Temperature uncertainty, δT, represents the smallest change in temperature that can be resolved in a given measurement; δT is expressed in K or ^{o}C and follows Eq.4:

$$\delta T = \frac{1}{S_{rel}} \frac{\delta LIR}{LIR} \tag{4}$$

However, δT can also be calculated in an experimental way. To obtain it, several measurements must be made at the same temperature. The variability of the calculated temperature is determined by using the fitted curve of the thermometer. The results show a Gaussian distribution, from which the mean and standard deviation (σ) values can be determined, those are related with the average temperature and uncertainty (δT), respectively[3][9].

5 Methodology

En la presente sección, se desarrolla el método utilizado para la fabricación de la muestra y evaluación de la muestra como sensor remoto de temperatura. En primer lugar, se explica el método de fabricación del material ópticamente activo, $Gd_3NbO_7 : Yb^{3+}, Tm^{3+}$, y el proceso de mezcla con la resina Simple Siraya Tech; A continuación se especifica el montaje experimental para los dos experimentos llevados a cabo en este tabajo: La medida del valor LIR para las emisiones de la muestra a 1626 y 1436 nm cuando se encuentra sumergida en 2-Propanol y la medida del LIR para las emisiones a 1626 y 831 nm cuando se encuentra sumergida en agua. Finalmente, se muestra el montaje utilizado para el aumento controlado de la temperatura.

5.1 Sample preparation

The synthesis method used in the materials of the present work has been the ceramic method assisted by high energy ball milling in zirconium oxide cuvettes, Fritsch model Pulverisette 7. The milling has been carried out from

the corresponding metal oxides, except for niobium which has been used niobium ammonium oxalate. To ensure stoichiometric weighing, the different oxides were heated at 900°C for 3 hours to eliminate any residual moisture or gases that may have been adsorbed and then stored in a desiccator. Regarding niobium ammonium oxalate, thermogravimetry has been performed considering that the product obtained is niobium oxide (V) (Nb_2O_5).

In a typical synthesis, each of the reagents is stoichiometrically weighed and added into a zirconium oxide cuvette. Then approximately 30 ml of isopropanol is added for every 5 grams of compound to be prepared plus 5 zirconium oxide spheres of different diameters. Once the precursors, isopropanol and the ceramic balls have been added, the whole assembly is introduced into the ball mill and 3 grinding cycles are applied at 800rpm for 30 minutes, with a stop of 5 minutes between each cycle. In addition, the direction of rotation is reversed after each cycle. After the grinding process has been applied, it is placed in a vacuum oven at 60 degrees and all the isopropanol is allowed to evaporate overnight.

The powder is then pressed into a pellet and placed in the oven for a first decomposition at 800^{o}C for 10h. Special care must be taken to place a layer of powder between the pellet and the alumina support to prevent possible contamination. The pellet is then ground and the same process is repeated but this time the sample is heated up to 1500°C for 24h. Once the treatment is finished, the pellet is ground and the final product of the synthesis is obtained.

The sample is composed of 2% Tm and 2%Yb, and the amounts weighed to prepare 2.5 grams were:

- MW(Gd2O3) (99%)= 2.0006 g
- MW(Yb2O3)(99%)= 0.0146 g
- MW(Tm2O3)(99%)= 0.0143 g
- MW[NAMOX, Nb2O5)](28.63%)= 1.7138

The optical active material $Gd_3NbO_7 : Yb^{3+}, Tm^{3+}$ was mixed with a Simple Siraya Tech resin, with a composition of urethane acrylate (CAS No.

877072-28-1, wt% = 20–50%), acrylic monomer (CAS No. 64401-02-1, wt% = 30–60%), and photoinitiator (CAS No. 119-61-9, wt% = 0–5%). It was then coupled to a 3D printed support and cured in an UV lamp at 365 nm.

The material employed for manufacturing the 3D printed support was a 3D850 SMARTFIL (from Smart Materials 3D) polylactic acid. The piece was designed using Tinkercad software, and the digital file was saved as surface tessellation language (STL) format. STL file was exported to Bambu Studio slicer for the selection of the manufacturing parameters. Finally, the specimen was printed, by fused deposition using a Bambu Lab X1 Carbon desktop printer. The manufacturing parameters were layer width of 0.4 mm, layer height of 0.2 mm, 100% infill pattern density, bed temperature of 50ºC, extruder temperature of 220ºC and deposition speed of 30 mm/s for the base and 25 mm/s for the sensor part.

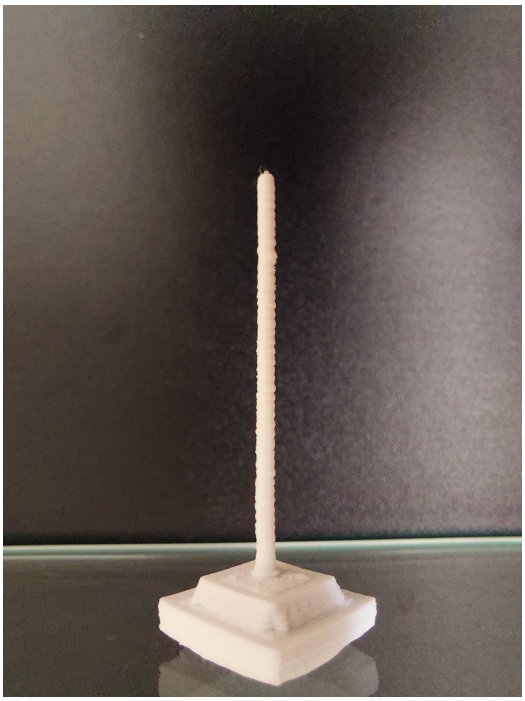

Figure 2: Mixture of $Gd_3NbO_7 : Yb^{3+}, Tm^{3+}$ and resin adhered to the 3D printed support.

5.2 Detection system

The sample adhered to the support is submerged in two different fluids: 2-Propanol (also known as isopropanol or propan-2-ol) and water. It is excited at 700 nm with a titanium-sapphire laser pumped at 532 nm Millenia eV105 Spectra Physics. The sample is excited with 100 mW power. It is heated in a controlled manner and the emission from the corresponding electronic transition is then detected with one (NIR) or two detectors (NIR and VIS), depending of the wavelength range needed, connected to an ANDOR spectrograph. Lastly, the signal is processed using OriginLab2024.

5.2.1 Experimental setup used for the measurements of the optical emissions of $Gd_3NbO_7 : Yb^{3+}, Tm^{3+}$ immersed in 2-Propanol

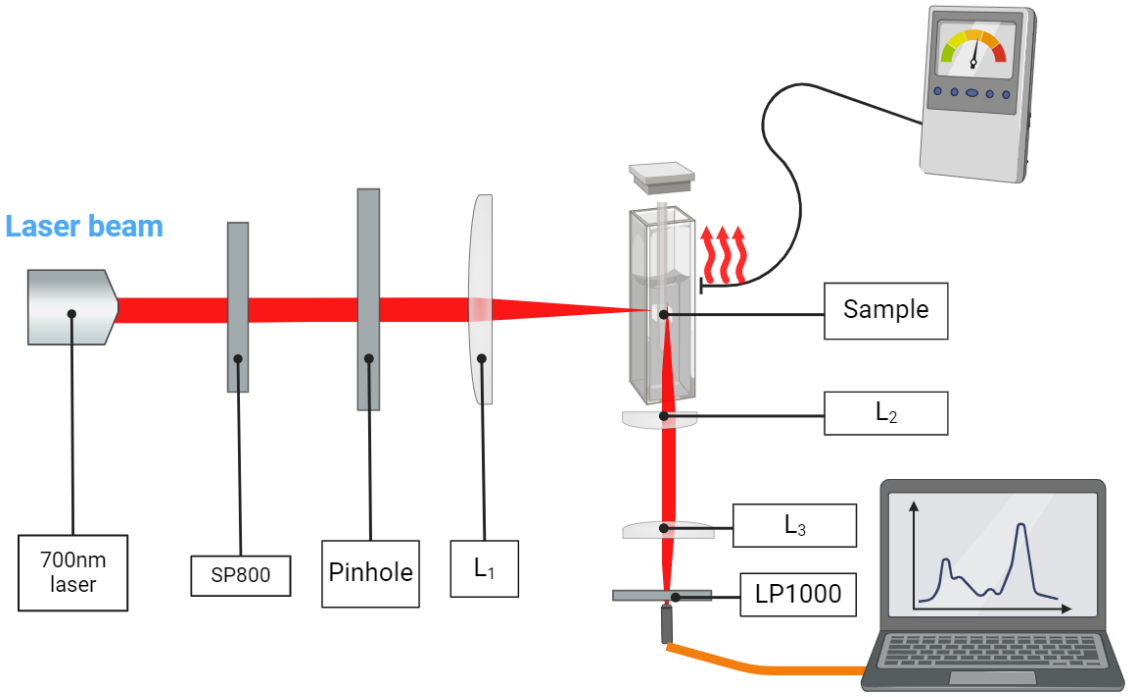

Figure 3: Experimental setup used for the measurements of the optical emissions of the $Gd_3NbO_7 : Yb^{3+}, Tm^{3+}$ sample immersed in 2-Propanol.

The sample is placed in a 2x2x8 cm quartz container to ensure optimal thermal transmission and a thermocouple is used to verify its temperature. To excite the sample, a laser tuned to 700ṅm is used. The intensities of the emissions at 1436 nm and 1626 nm are measured using a NIR detector. The detection time is 1.5 s. The temperature of the sample is gradually increased until it reaches 49ºC. While the temperature is rising, 15 emissions of the sample are measured approximately every 2ºC to determine the ratio dependence on temperature and to calculate the relative thermal sensitivity (S_{Rel}); Finally, at a fixed temperature, 100 measurements are obtained the temperature uncertainty (δT) of the sensor, as described in Eq.4.

5.2.2 Experimental setup used for the measurements of the optical emissions of $Gd_3NbO_7 : Yb^{3+}, Tm^{3+}$ immersed in water

Similar to the procedure when the sample is immersed in 2-Propanol, it is placed inside a cuvette and excited at 700 nm. However, this time we focus on analyzing the emissions at 831nm and 1626nm. Because of that, it is necessary the use of two detectors, a VIS one and a NIR one, with 1 and 5s exposure time, respectively; Subsequently, the temperature of the sample was gradually increased to ensure thermal stability until it reached 49.5ºC. During this process, 15 measurements were taken for subsequent use in LIR and S_{Rel} calculations. Finally, 100 measurements are obtained at a fixed temperature to determine the temperature uncertainty δT, as described in Eq.3.

Due to water absorption[12], the emission at 1436 nm completely disappears from the detected emission spectrum. For this reason, in water, the 831 nm emission is used to calculate the intensity ratio versus the 1626 nm emission. This one is also attenuated by water absorption, yet the signal intensity remains strong enough to be measurable.

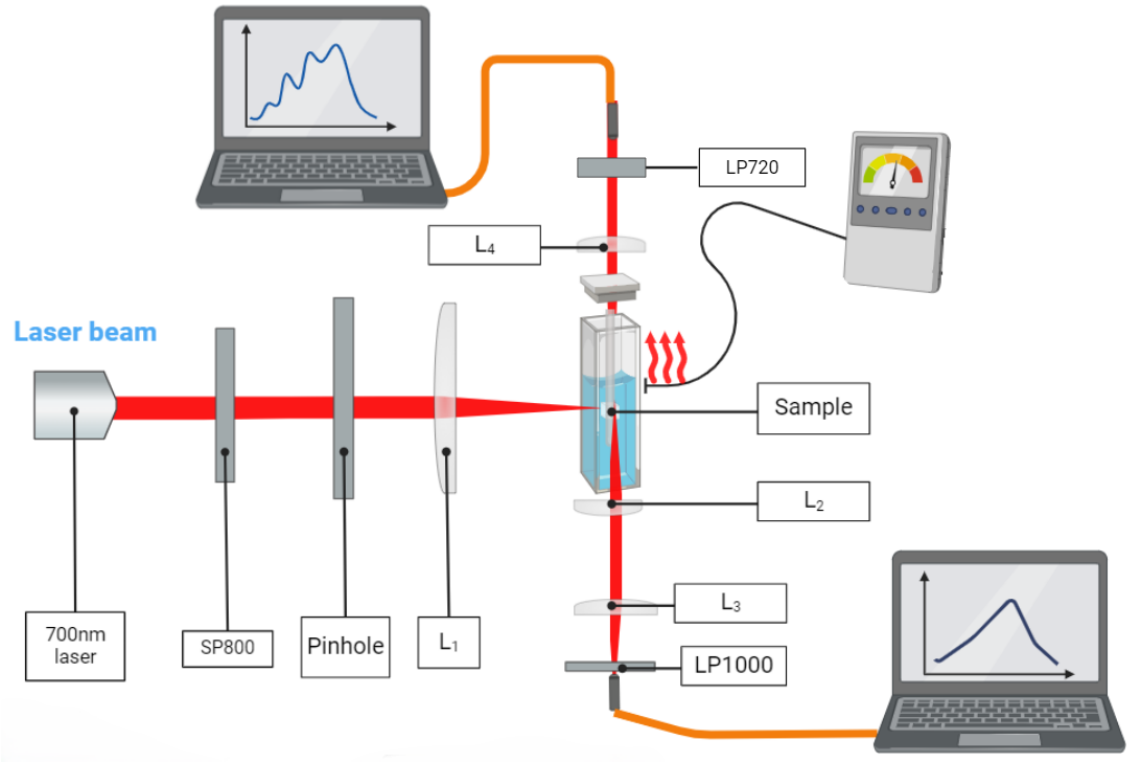

Figure 4: Experimental setup used for the measurements of the optical emissions of the $Gd_3NbO_7 : Yb^{3+}, Tm^{3+}$ sample immersed in water.

5.3 Heating system

The sample is inserted in a small quartz container, to ensure better heat transmission, filled with the fluid of choice. It is then heated up using a thermal bath. A thermocouple is connected to the container for a more precise scale. Fig.5 shows the heating system:

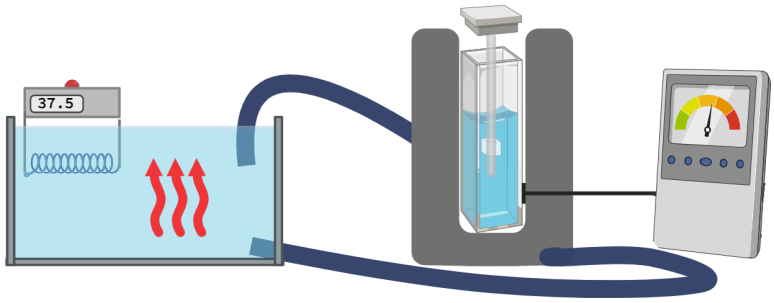

Figure 5: Experimental Setup of the heating system used in these experiments.

6 Results

En este apartado, se presentan los resultados obtenidos en este trabajo. En primer lugar, se identifican las emisiones a 831, 1436 y 1626 nm detectadas en el espectro del $Gd_3NbO_7 : Yb^{3+}, Tm^{3+}$ *con las siguientes transiciones electrónicas del* Tm^{3+}*:* $^3\mathrm{H}_4 \rightarrow ^3\mathrm{H}_6$*,* $^3\mathrm{H}_4 \rightarrow ^3\mathrm{F}_4$ *y* $^3\mathrm{F}_4 \rightarrow ^3\mathrm{H}_6$*, respectivamente, y se explican los diferentes procesos involucrados en dichas transiciones; Posteriormente, se calcula el LIR entre las emisiones de 1436 y 1626 nm cuando la muestra se encuentra sumergida en propanol, la sensitividad térmica relativa y la incertidumbre térmica del sensor; Finalmente, siguiendo el mismo proceso, con la diferencia de utilizar la emisión a 831 nm en lugar de la emisión a 1436 nm para calcular LIR. Se calcula también la sensitividad térmica relativa y la incertidumbre térmica para este experimento, con el objetivo de evaluar el desempeño del sensor en agua.*

6.1 Luminescence of $Gd_3NbO_7 : Yb^{3+}, Tm^{3+}$

This study focus in the emissions of the $Gd_3NbO_7 : Yb^{3+}, Tm^{3+}$ sample coming from Tm^{3+} emissions when it is excited at 700 nm.

Among the various Tm^{3+} emissions observable under this excitation, this work focuses on the emissions at 831 nm, 1436 nm, and 1626 nm. Upon excitation at 700 nm, electrons initially populate the $^3F_3$ and $^3F_2$ levels of Tm^{3+}, subsequently undergoing non-radiative (or phononic) transition to the $^3H_4$ level. The 831 nm emission occurs as the electrons transition directly to the ground state. Instead, for the 1436 nm and 1626 nm emissions, the process involves an initial $^3H_4 \rightarrow ^3 F_4$ (1436 nm) transition, followed by a $^3F_4 \rightarrow ^3 H_6$ transition (1626 nm) to the ground state, as illustrated in Fig.6:

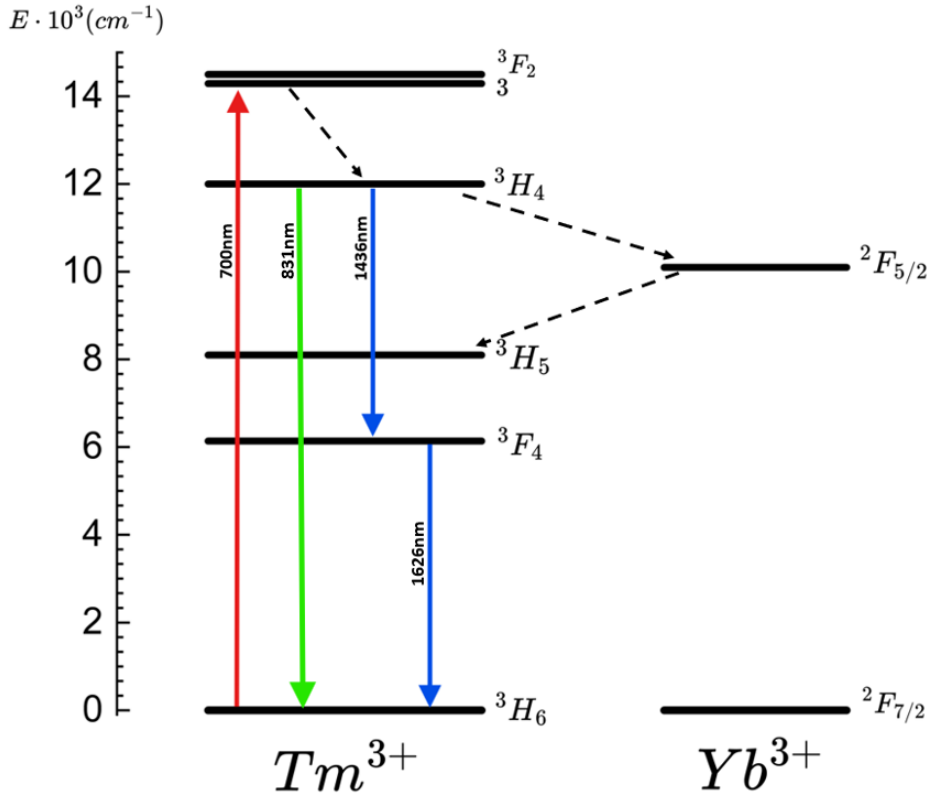

Figure 6: Partial energy level diagram of Tm^{3+} and Yb^{3+} ions indicating the involved transitions.

Two things can be noted about the transitions previously described. First, they do not correspond to Tm^{3+} TCLs. Secondly, the laser used for the excitation (700 nm) and the emissions at 831 nm and 1626 nm fall within biological windows [BW-I (650-950 nm) and BW-III (1500-1800 nm)[3]], making the measure between these transitions more suitable for biological applications compared to those using the emission at 1436 nm.

Often in the literature, a matrix doped with Tm^{3+} and Yb^{3+} uses the last one as a sensitizer to improve the luminescence of the former. However, for this technique the excitation must be around 980 nm, leaving it outside the biological windows[3][11]. For this reason, the sample is excited at 700nm in this work. The Yb^{3+} is present in the sample of the current experiments and might affect via non-radiative decay processes, nevertheless, it is not excited by the laser nor measured. Thus, being the Tm^{3+} the only relevant ion.

6.2 Luminescence of the sample immersed in 2-Propanol

The sample is inmersed in 2-propanol, and the emission bands at 1436 nm and 1626 nm are measured as a function of temperature from 22.8^{o}C to 49.4^{o}C.

In Fig.7, is shown the simplified energy level diagram and the emissions obtained under excitation at 700 nm when the sample is inmersed in 2-Propanol; The emission spectra corresponding to the $^3H_4 \rightarrow ^3F_4$ and $^3F_4 \rightarrow ^3H_6$ transitions are presented in Fig.7 (b), while temperature is increased from 22.8^{o}C to 49.4^{o}C. As observed, I_{1436} decreases with rising temperature, whereas I_{1626} increases.

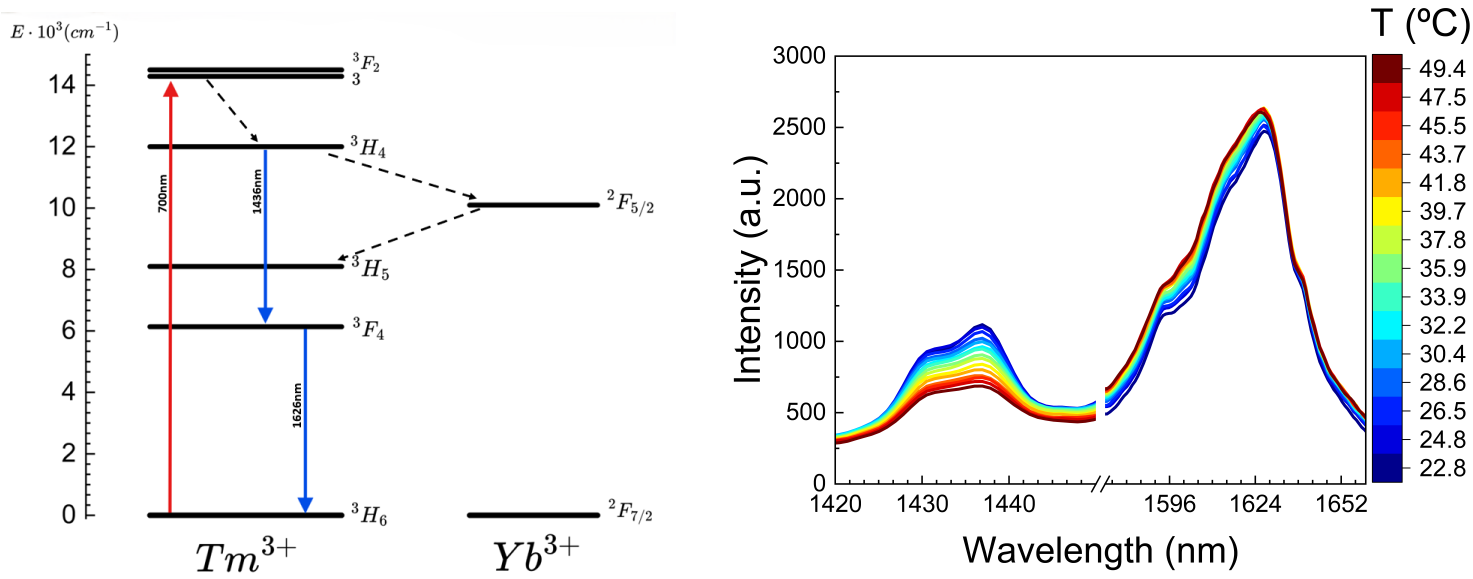

Figure 7: (a) Simplified energy level diagram and involved transitions. (b) Emission spectra obtained as function of temperature when the sample is immersed in 2-Propanol.

6.2.1 Luminescense Intensity Ratio

Following the results obtained in the previous section, the ratio between the intesities (LIR) at 1626 nm and 831 nm is presented in Fig.8. Given the non-TCLs nature of this levels, the LIR values are fitted to an exponential equation, and the fitting parameters are:

$$LIR(T) = 0.50357 + 1.79995 * exp(0.0177 * T) \tag{5}$$

Note that, as the data does not follow the typical Boltzmann-type equation used for TCLs, the fitting parameters obtained are purely experimental.

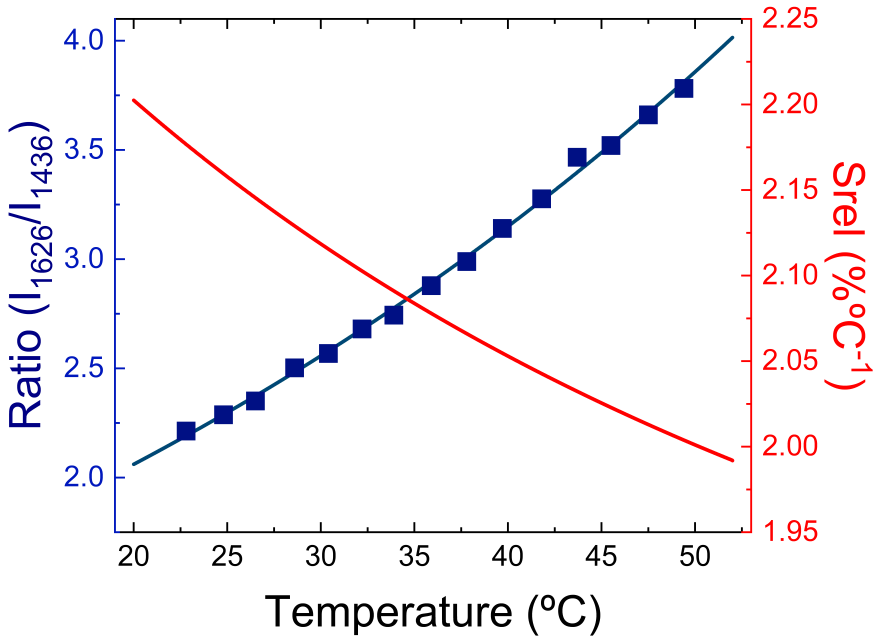

Figure 8: LIR experimental values (square dots), fitting (blue line) and corresponding S_{Rel} (red line) of the mixture of Gd_3NbO_7 : Yb^{3+}, Tm^{3+} with Siraya resin immersed in 2-Propanol.

In Fig.8, a change in LIR is observed, ranging from 2 to 4 in the temperature range from 22.8ºC to 49.4ºC.

6.2.2 Sensor performance

In Fig.8, is also represented the Relative Thermal Sensitivity S_{Rel}, Eq.3. The maximum value in S_{Rel} is used to compare thermometers independently of their nature or material employed; For this specific experiment, $S_{Rel} = 2.2\%ºC^{-1}$ at 22.8ºC (295.95K), a value considered high sensitivity in biological applications[5].

To find the temperature uncertainty δT, 100 measures are taken at a fixed temperature. The ratios of I_{1626} versus I_{1436} are obtained and, using the fitting curve, the Gaussian distribution of the variability in the calculated temperature is represented in Fig.9. The standard deviation σ is equivalent to δT and the value obtained is 0.5ºC.

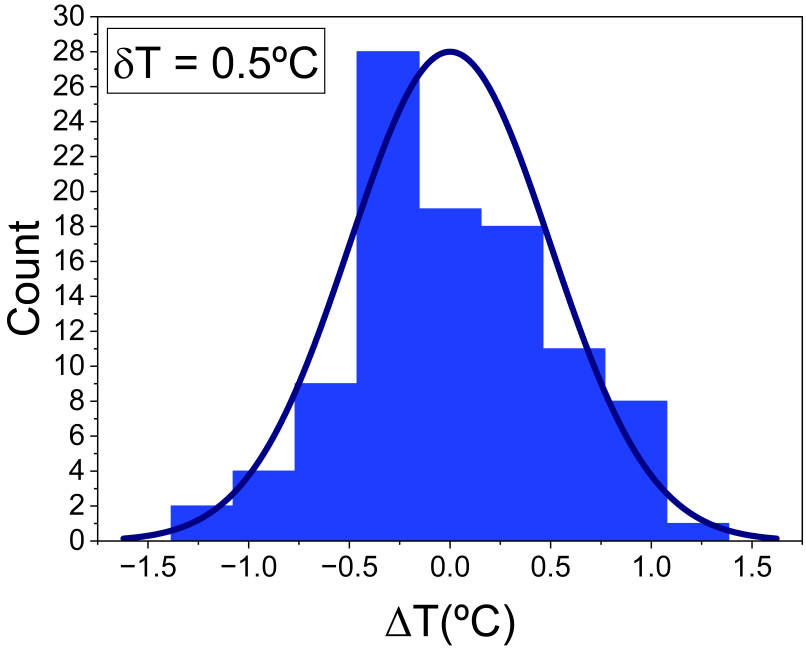

Figure 9: Temperature uncertainty when the sample is submerged in 2-Propanol.

To the best of our knowledge, this has been the first time the ratio, between the 1436 nm ($^3H_4 \rightarrow ^3 F_4$) and 1626 nm ($^3F_4 \rightarrow ^3 H_6$) emission bands of Tm^{3+}, has been studied as a function of temperature. The relative thermal sensitivity obtained shows high values $S_{Rel} > 2\%$ with a thermal uncertainty δT of 0.499ºC. As conclusion, this temperature sensor can used in many applications where the 2-Propanol is widely used as solvent. As example, in cosmetics, perfumes and hygiene products, the production of medicines,chemistry reactions and synthesis processes[13]. However, the use of the emission line at 1436 nm hinds the utilization of this specific experi-

ment in biological applications.

6.3 Luminescence of the sample immersed in water

To evaluate the thermal capabilities of the sample while it is submerged in water, the emission bands at 831 nm and 1626 nm are measured as a function of temperature for a range between 21ºC and 49.5ºC.

In Fig.10, it is shown a simplified energy diagram and the emissions measured when the sample is excited at 700nm while the sample is immersed in water; The spectra of said emissions can be observed in Fig.?? (b) and correspond to the following transitions, respectively: ^{3}H$_4$ $\rightarrow^3$ H$_6$ and ^{3}F$_4$ $\rightarrow^3$ H$_6$. As observed, I_{831} decreases with rising temperature, whereas I_{1626} increases.

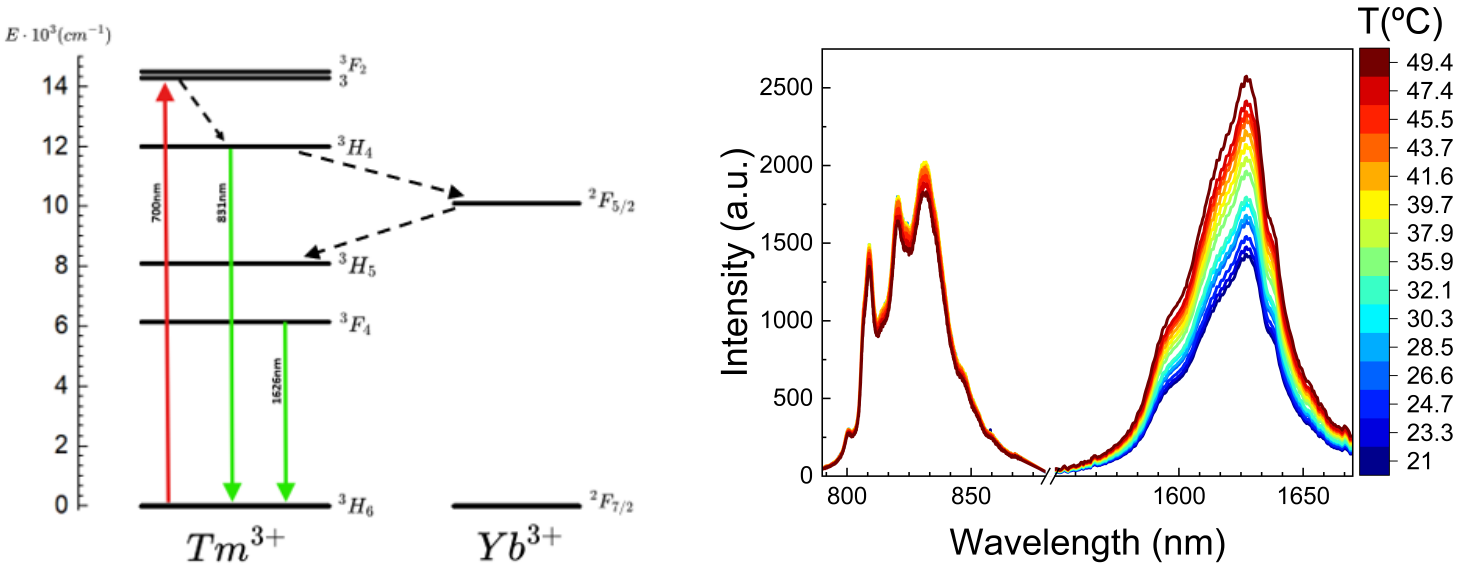

Figure 10: (a) Simplified energy level diagram and involved transitions. (b) Emission spectra obtained as function of temperature when the sample is immersed in water.

6.3.1 Luminescence Intensity Ratio

To calculate LIR, the ratio between the intensities I_{1626} and I_{831} is used and fitted using an exponential fit, Eq.6; The results obtained are shown in Fig.11:

$$LIR(T) = 0.48069 + 0.10544 * exp(0.04349 * T) \quad (6)$$

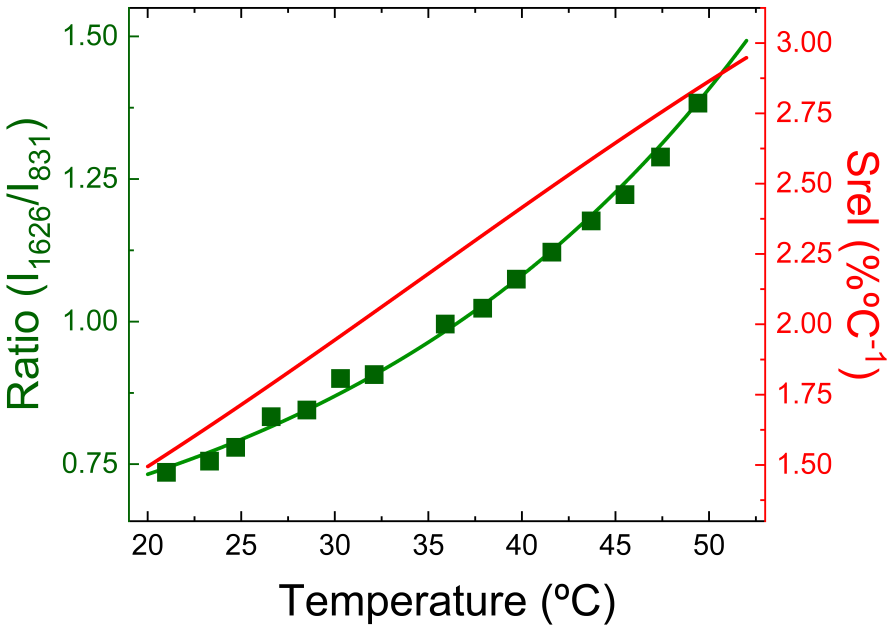

Figure 11: LIR experimental values (square dots), fitting (green line) and corresponding S_{Rel} (red line) of the mixture of $Gd_3NbO_7 : Yb^{3+}, Tm^{3+}$ with Siraya resin immersed in water.

6.3.2 Sensor performance

In Fig.11, is also represented the Relative Thermal Sensitivity S_{Rel}, Eq.3. The maximum value in S_{Rel} is used to compare thermometers independently of their nature or material employed.

For this specific experiment, $S_{Rel} = 2.8\%\ ^{o}C^{-1}$ at 49.5ºC (322.65K), among the highest obtained in the related literature for biological applications[5][3].

To find the temperature uncertainty δT, 100 measures are taken at a fixed temperature. The ratios of I_{1626} versus I_{831} are obtained and, using the fitting curve, the Gaussian distribution of the variability in the calculated temperature is represented in Fig.12. The standard deviation σ is equivalent to δT and the value obtained is 0.2ºC.

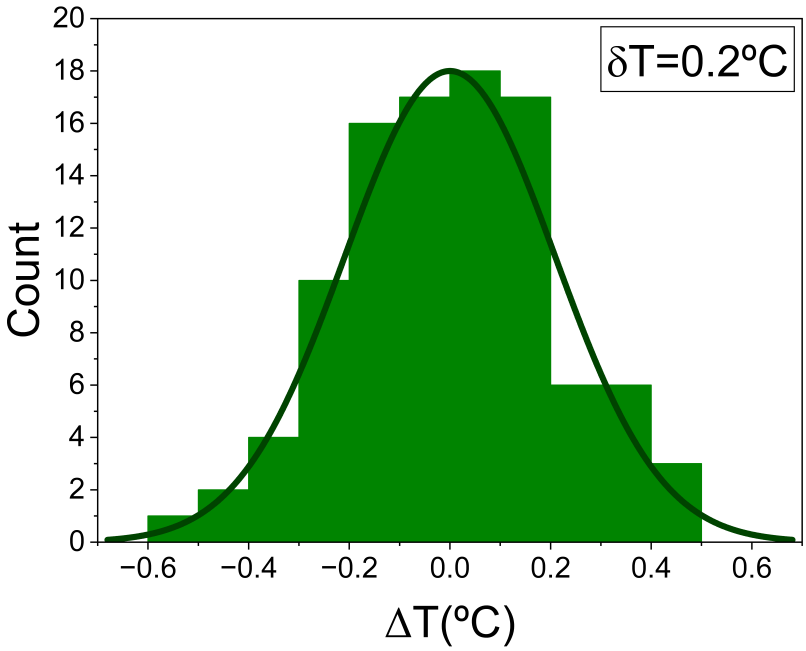

Figure 12: Temperature uncertainty when the sample is submerged in water.

To the best of our knowledge, this has been the first time the ratio, between the 831 nm ($^3H_4 \rightarrow ^3 H_6$) and 1626 nm ($^3F_4 \rightarrow ^3 H_6$) emission bands of Tm^{3+}, has been studied as a function of temperature.

In this experiment, both the laser employed to excite the sample (700 nm) and the emissions measured (831 and 1626 nm) fall within biological windows,

BW-I, BW-I and BW-III respectively. Thus, making it a better suit for biological applications than the previous experiment.

The sensor immersed in water showed a LIR with a significant increase from 0.7 to 1.5 in the temperature range studied (21-49.5^{o}C). Yet, water absorbance hinds the detection of the 1626 nm emission[12], especially at lower temperatures.

Furthermore, it should be noticed that, given the nature of the levels used for both experiments, the S_{Rel} should be the same in both cases, however, it can be observed in Fig.9 and Fig.12 that this is not the case. The difference, can be attributed to the different shifts that occurs in the mediums, and that can also affect the intensity of the different levels[14][15].

According to Nexha. A *et Al.*[3], out of 149 papers cited that are meant to study luminescence thermometers in the biological windows, only 45% excite the sample with a laser that falls within a biological window and 8 have a S_{Rel} $>2\%^{o}C^{-1}$. Thus, considering both the wavelength of the excitation used and the $S_{Rel} = 2.8\%^{o}C^{-1}$ obtained in water, the sample of $Gd_3NbO_7 : Yb^{3+}, Tm^{3+}$ resin gives a better suited result for biological applications than 95% of said review examples, while having a thermal uncertainty δT of 0.2^{o}C.

7 Conclusions

Finalmente, en esta sección se enuncian las conclusiones de los experimentos realizados.
Primeramente, se hace conocer que el material ópticamente activo, $Gd_3NbO_7 : Yb^{3+}, Tm^{3+}$, fue sintetizado con éxito y mezclado con la resina Simple Siraya Tech; Se estudió la emisión de esta muestra, consiguiendo medir la dependencia de la relación entre sus intensidades con la temperatura cuando esta se encontraba sumergida en 2-Propanol y agua; Se obtiene valores considerados altos para las sensitividades térmicas relativas de ambos experimentos. Según nuestro conocimiento, es la primera vez que los non-TCLs de Tm^{3+} utilizados en ambos experimentos realizados en este trabajo han sido analizados en función de la temperatura, y se concluye que los resultados demuestran que nuestra muestra en un buen candidato a sensor remoto de temperaura dentro de los rangos biológicos, con el añadido de poder ser fabricado en diversas formas debido a ser incluido en una resina típicamente destinada a la impresión 3D.

The aim of the work is to study the thermal capabilities of a sensor fabricated by the combination of Gd_3NbO_7 doped with Tm^{3+} and Yb^{3+} and Simple Siraya Tech resin, while submerged in two fluids, 2-Propanol and water.

The optical active material, $Gd_3NbO_7 : Yb^{3+}, Tm^{3+}$ was successfully synthesized and mixed with Simple Siraya Tech resin, a common resin typical in 3D printing. Thus, creating a sample whose luminescence can be used for imaging and temperature sensing, that can also be fabricated according to the needs of the application thanks to the mixtures with the 3D resin. When excited under 700 nm laser, the sample showed the typical emission bands in 1626 nm, 1436 nm and 831nm, that were identified as the following transitions realted to Tm^{3+}: $^3F_4 \rightarrow^3 H_6$, $^3H_4 \rightarrow^3 F_4$ and $^3H_4 \rightarrow^3 H_6$, respectively. Given that both, the excitation wavelength and most of the emitted bands, lay within the known as biological windows (BW-I, BW-III and BW-I), we proceed to study the material in different mediums typically

used in biological applications.

First, the sample was immersed in 2-propanol and the ratio (LIR) of emission bands at 1626 nm and 1436 nm was recorded as a function of temperature in a range between 22.8ºC and 49.4ºC. It was observed that, while the emission from the 1436 nm band decreased with increasing temperature, the intensity of the 1626 nm band increased. This lead to a maximum Relative Thermal Sensitivity (S_{Rel}) of up to $2.2\%^{o}C^{-1}$ at 22.8ºC (295.95K). When compared to other values from the related literature, this maximum is among the highest ever recorded. Experimental temperature Uncertainty was also obtained with a minimum of 0.5ºC.

Secondly, the $Gd_3NbO_7 : Yb^{3+}, Tm^{3+}$ mixed with resin was submerged in water where the emissions at 831nm and 1626 nm were detected when the sample was excited with a 700 nm laser, falling all of them within a biological window (BW-I, BW-III and BW-I respectively). LIR measurements were recorded in a range of 21ºC to 49.5ºC. Similarly to the case of 2-propanol, the 831 nm emission slightly decrease with increasing temperature while the 1626 nm increased. The calculated Relative Thermal Sensitivity (S_{Rel}) lead to a maximum of $2.8\%^{o}C^{-1}$, also among the highest recorded. Temperature uncertainty was also obtained with a minimum of 0.2ºC.

To summarize, it has been studied for the first time the LIR values of the Tm^{3+} non-TCLs for 1626 nm, 1436 nm and 831nm. These levels, have shown a great performance for temperature sensing within the biological temperature range in both 2-Propanol and water mediums. Furthermore, the material used combined a mixture of $Gd_3NbO_7 : Yb^{3+}, Tm^{3+}$ and 3D printing resin, thus making it a very malleable material, that can be fabricated in various shapes according to the requirements of the application. Overall, all of these properties that this material bring to the table make it a great candidate for, not only biological but any application that requires remote very senstivitive temperature sensing.

References

[1] J.-C. G. Bünzli, "Chapter 287 - lanthanide luminescence: From a mystery to rationalization, understanding, and applications," in *Including Actinides*, ser. Handbook on the Physics and Chemistry of Rare Earths, J.-C. G. Bünzli and V. K. Pecharsky, Eds., vol. 50, Elsevier, 2016, pp. 141–176. DOI: https://doi.org/10.1016/bs.hpcre.2016.08.003. [Online]. Available: https://www.sciencedirect.com/science/article/pii/S016812731630023X.

[2] A. E. Albers, E. M. Chan, P. M. McBride, C. M. Ajo-Franklin, B. E. Cohen, and B. A. Helms, "Dual-emitting quantum dot/quantum rod-based nanothermometers with enhanced response and sensitivity in live cells," *Journal of the American Chemical Society*, vol. 134, no. 23, pp. 9565–9568, 2012, PMID: 22642769. DOI: 10.1021/ja302290e. eprint: https://doi.org/10.1021/ja302290e. [Online]. Available: https://doi.org/10.1021/ja302290e.

[3] A. Nexha, J. J. Carvajal, M. C. Pujol, F. Díaz, and M. Aguiló, "Lanthanide doped luminescence nanothermometers in the biological windows: Strategies and applications," *Nanoscale*, vol. 13, pp. 7913–7987, 17 2021. DOI: 10.1039/D0NR09150B. [Online]. Available: http://dx.doi.org/10.1039/D0NR09150B.

[4] E. C. Ximendes, U. Rocha, T. O. Sales, *et al.*, "In vivo subcutaneous thermal video recording by supersensitive infrared nanothermometers," *Advanced Functional Materials*, vol. 27, no. 38, p. 1 702 249, 2017. DOI: https://doi.org/10.1002/adfm.201702249. eprint: https://onlinelibrary.wiley.com/doi/pdf/10.1002/adfm.201702249. [Online]. Available: https://onlinelibrary.wiley.com/doi/abs/10.1002/adfm.201702249.

[5] A. Bednarkiewicz, L. Marciniak, L. D. Carlos, and D. Jaque, "Standardizing luminescence nanothermometry for biomedical applications," *Nanoscale*, vol. 12, pp. 14 405–14 421, 27 2020. DOI: 10.1039/D0NR03568H. [Online]. Available: http://dx.doi.org/10.1039/D0NR03568H.

[6] C. Hernández-Álvarez, P. I. Martín-Hernández, I. R. Martín, *et al.*, "Optical temperature sensor evaluation in a working gear motor: Application of luminescence thermometry in industrial technology," *Ad-*

vanced Optical Materials, vol. 12, no. 17, p. 2 303 328, 2024. DOI: https://doi.org/10.1002/adom.202303328. eprint: https://onlinelibrary.wiley.com/doi/pdf/10.1002/adom.202303328. [Online]. Available: https://onlinelibrary.wiley.com/doi/abs/10.1002/adom.202303328.

[7] W. Koechner and M. Bass, *Solid-State Lasers : A Graduate text*. Apr. 2013. [Online]. Available: https://ci.nii.ac.jp/ncid/BA6256924X.

[8] M. H. Werts, "Making sense of Lanthanide Luminescence," *Science progress*, vol. 88, no. 2, pp. 101–131, May 2005. DOI: 10.3184/003685005783238435. [Online]. Available: https://doi.org/10.3184/003685005783238435.

[9] J. J. C. Martí and M. C. P. Baiges, *Luminescent thermometry*. Springer, May 2024.

[10] M. Runowski, P. Woźny, N. Stopikowska, I. R. Martín, V. Lavín, and S. Lis, "Luminescent nanothermometer operating at very high temperature—sensing up to 1000 k with upconverting nanoparticles (yb3+/tm3+)," *ACS Applied Materials & Interfaces*, vol. 12, no. 39, pp. 43 933–43 941, 2020, PMID: 32869638. DOI: 10.1021/acsami.0c13011. eprint: https://doi.org/10.1021/acsami.0c13011. [Online]. Available: https://doi.org/10.1021/acsami.0c13011.

[11] C. Wang, Y. Jin, R. Zhang, Q. Yao, and Y. Hu, "A review and outlook of ratiometric optical thermometer based on thermally coupled levels and non-thermally coupled levels," *Journal of Alloys and Compounds*, vol. 894, p. 162 494, 2022, ISSN: 0925-8388. DOI: https://doi.org/10.1016/j.jallcom.2021.162494. [Online]. Available: https://www.sciencedirect.com/science/article/pii/S0925838821039049.

[12] 邓孺孺, 何颖清, 秦雁, 陈启东, and 陈蕾, "85900—2500nm85," 遥感学报, vol. 16, no. 1, pp. 192–206, 2012. DOI: 10.11834/jrs.20121188.

[13] [Online]. Available: https://ec.europa.eu/growth/tools-databases/cosing/details/34680.

[14] T. Muñoz-Ortiz, L. Abiven, R. Marin, *et al.*, "Temperature dependence of water absorption in the biological windows and its impact on the performance of ag2s luminescent nanothermometers," *Particle & Particle Systems Characterization*, vol. 39, no. 11, p. 2 200 100, 2022. DOI: https://doi.org/10.1002/ppsc.202200100. eprint: https://onlinelibrary.wiley.com/doi/pdf/10.1002/ppsc.202200100.

[Online]. Available: https://onlinelibrary.wiley.com/doi/abs/10.1002/ppsc.202200100.

[15] W. A. P. Luck and W. Ditter, *Zeitschrift für Naturforschung B*, vol. 24, no. 5, pp. 482–494, 1969. DOI: doi:10.1515/znb-1969-0502. [Online]. Available: https://doi.org/10.1515/znb-1969-0502.